

See discussions, stats, and author profiles for this publication at: <https://www.researchgate.net/publication/231645461>

Band Gap Narrowing versus Formation of Electronic States in the Gap in N–TiO₂ Thin Films

ARTICLE *in* THE JOURNAL OF PHYSICAL CHEMISTRY C · DECEMBER 2010

Impact Factor: 4.77 · DOI: 10.1021/jp104634j

CITATIONS

18

READS

24

7 AUTHORS, INCLUDING:



Said Hamad Gomez

Universidad Pablo de Olavide

60 PUBLICATIONS 1,269 CITATIONS

SEE PROFILE



Juan Pedro Espinós

Spanish National Research Council

190 PUBLICATIONS 3,404 CITATIONS

SEE PROFILE



José Cotrino

Universidad de Sevilla

110 PUBLICATIONS 1,307 CITATIONS

SEE PROFILE



Agustin R. Gonzalez-Elipse

Spanish National Research Council

432 PUBLICATIONS 7,209 CITATIONS

SEE PROFILE

Band Gap Narrowing versus Formation of Electronic States in the Gap in N–TiO₂ Thin Films

P. Romero-Gómez,[†] Said Hamad,[§] J. C. González,[†] A. Barranco,[†] J. P. Espinós,^{†,‡} J. Cotrino,^{†,‡} and A. R. González-Elipe^{*,†}

Instituto de Ciencia de Materiales de Sevilla (CSIC-Universidad de Sevilla), Avenida Américo Vespucio 49, 41092 Sevilla, Spain, Departamento de Física Atómica, Molecular y Nuclear, Universidad de Sevilla, Avenida Reina Mercedes 49, 41012 Sevilla, Spain, and Department of Physical, Chemical and Natural Sciences, Universidad Pablo de Olavide, Carretera de Utrera, km 1, Sevilla, Spain

Received: May 20, 2010; Revised Manuscript Received: October 17, 2010

N-containing TiO₂ thin films with different amounts of nitrogen have been prepared by plasma enhanced chemical vapor deposition (PECVD) by using different titanium precursors without (titanium isopropoxide, TTIP) and with (tetrakis diethylamino titanium, TDEAT and tetrakis dimethylamino titanium, TDMAT) nitrogen in their structures and different N₂/O₂ ratios as plasma gas. For low/high content of nitrogen, Ti–NO- and/or Ti–N-like species have been detected in the films by X-ray photoelectron spectroscopy (XPS). Their optical behavior is characterized by a red shift of their absorption edge when Ti–N species are a majority, and by an unmodified edge with localized absorption states in the gap when only Ti–NO-like species are present in the film. The experimental results have been interpreted by calculating the density of states of model systems consisting of a 2 × 2 × 3 repetition of the anatase unit cell. This basic structure incorporates nitrogen defects in either substitutional or interstitial lattice positions that are considered equivalent to the Ti–N- and Ti–NO-like species detected by XPS. To simulate the effect of, respectively, a low or a high concentration of nitrogen, calculations have been carried out by placing two nitrogen defects either in separated or in nearby positions of the anatase structure. The computational analysis reveals that the defects have different stabilization energies and confirm that an edge shift of the valence band is induced by the substitutional nitrogen centers, as observed when a high concentration of Ti–N species becomes incorporated into the films. In agreement with the experimental results, when only Ti–NO like species are detected by XPS, no band gap narrowing is obtained by the calculations that predict the appearance of localized electronic states in the gap. The fact that only these latter films present water wetting angle photoactivity when irradiated with visible light supports that the presence of Ti–NO-like species is a required condition for visible light photoactivity.

1. Introduction

N-modified TiO₂ materials have been widely studied during the past years because of the possibility of making them photocatalytically active under visible light illumination. Since the seminal work of Asahi et al.,¹ many papers have appeared in the literature trying to unravel the reasons that sustain this behavior.^{2–10} Of particular relevance in this regard are the recent works by Di Valentin et al.^{11–15} where, by combining theory and experiments mainly by EPR, they show that the species responsible for the visible photoactivity of N-containing TiO₂ consist of N atoms located in interstitial lattice positions where it bonds to Ti atoms and interacts with a nearby O ion of the lattice (i.e., a kind of Ti–NO species). This model contrasts with more traditional views linking the visible photoactivity of N-doped TiO₂ with the formation of substitutional nitrogen species (i.e., a kind of Ti–N species).^{1,5,16} Another related aspect that has generated much discussion within this topic is the influence of the incorporated nitrogen on the optical properties of the materials, namely in the changes in light absorption due

to possible modifications of the band gap of the titanium oxide.^{17–21} The appearance of absorption features in the visible region of the spectra of N-containing TiO₂ is generally taken as a required but not sufficient condition for visible photoactivity.²² However, the physical causes of this visible absorption are also controversial, with some authors supporting that the effect of the nitrogen species is to shift the band gap of the titanium oxide toward the visible,^{17–20} and others claiming that these species do not modify the band gap of the oxide but induce some electronic states in the band gap region that give rise to localized absorption features close to the absorption edge of the titanium oxide.^{11–15,22–24}

In a recent work on N-doped TiO₂ thin films prepared by plasma and evaporation methods, we have shown that, while Ti–NO species are able to induce some visible light decrease of the wetting angle of the surface,²² Ti–N species do not induce any kind of visible light activation. However, for the samples to present photocatalytic activity toward the photodegradation of dyes, it was required that besides Ti–NO species, the films were crystalline with a mixture of anatase and rutile. In this previous investigation we already noted that the absorption spectra of films with a high content of nitrogen depicted some absorption features in the visible, although no correlation could be established between the nitrogen content and the characteristics of the ultraviolet–visible (UV–vis) absorption spectra.

* To whom correspondence should be addressed. E-mail: arge@icmse.csic.es.

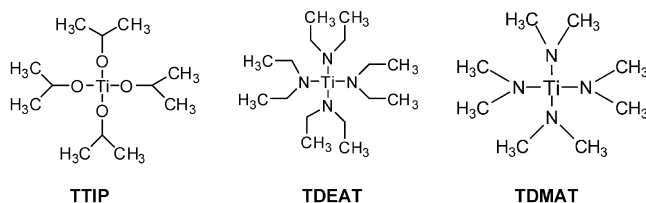
[†] CSIC-Universidad de Sevilla.

[‡] Departamento de Física Atómica, Molecular y Nuclear, Universidad de Sevilla.

[§] Universidad Pablo de Olavide.

As a continuation of this previous work, herein we primarily aim to determine whether each kind of nitrogen species (i.e., Ti-NO or Ti-N) has a specific effect on the physical causes (i.e., gap narrowing or development of localized states in the gap) determining the changes in the absorption spectra of N containing titanium oxide thin films (in the following, named as N-TiO₂ although changes in the Ti/O ratio may occur as a consequence of the formation of oxygen vacancies associated with the incorporation of Ti-N species²⁵). We approach this problem first by experimentally investigating a series of N-TiO₂ thin films where we have systematically changed the type and concentration of nitrogen species. To get such an ample set of samples with different concentrations of nitrogen species, we have employed the plasma enhanced chemical vapor deposition (PECVD) procedure and systematically modified the plasma conditions and other working parameters such as the type of precursor and temperature of the substrate. Such an experimental approach has hitherto not been widely used for the preparation of photoactive N-TiO₂ thin films, although the preparation of photoactive nanoparticles by atmospheric plasma deposition has been reported.²⁶ The most common titanium precursor used for the PECVD synthesis of TiO₂ thin films is titanium isopropoxide (TTIP).^{23,27–30} Tetrakis dimethylamino titanium (TDMAT) and tetrakis diethylamido titanium (TDEAT)^{31–33} are other two precursors that are used for the preparation of optical thin films. Therefore, another innovative approach of our work is the use of three titanium precursors (TTIP, TDEAT, and TDMAT) with the idea that the presence of direct Ti-N bonds in the structure of two of them and, very likely, their different reactivity, permit one to tune the state of nitrogen in the films and to control film properties such as UV-vis absorption spectra and photoactivity.

To account for the different experimental findings and particularly for the changes in the absorption spectra depending on the type and concentration of nitrogen species in the prepared N-TiO₂ thin films, we have theoretically modeled the electronic structure of these materials by calculating the density of states (DOS) of N-modified anatase for three different types of N defects incorporated in its structure. Modeling the Ti-NO (and Ti-ON as a possible alternative) defect states is done by assuming that N occupies an interstitial position and interacts with both oxygen and titanium ions of the lattice. This species, with nitrogen bearing a formal charge of -1 (i.e., NO³⁻-like species), could be described as a (NO)_O¹ defect center according to the Kröger-Vink notation of defect states in oxides. To simulate the Ti-N species, nitrogen substitutionally replaces an oxygen of the lattice and bonds directly to titanium in a kind of nitride species (i.e., N³⁻ species or N_O¹ according to the Kröger-Vink notation). Similar calculations simulating the effect of Ti-N- and Ti-NO-like species can be found in the works by Di Valentin et al.^{11,15} and Graciani et al.^{25,34} Herein, besides studying the stability of Ti-ON-like species, we have simulated the effect of the concentration of Ti-N or Ti-NO species on the optical properties of N-TiO₂ materials, an aspect that had not been addressed in these previous theoretical works. For this purpose, calculations have been carried out by placing two defect states quite separated (i.e., simulating a low concentration of nitrogen) or in nearby positions of the structure (i.e., simulating a high concentration of nitrogen), in this latter case making it possible that the two defect states interact between them as would be the case in samples with a high concentration of nitrogen species. The DOS calculations and particularly the analysis of the partial DOS plots of N, Ti, and O have confirmed the experimental findings and show that the incorporation of a



TTIP: titanium tetrakis isopropoxide

TDEAT: tetrakis diethyl amino titanium

TDMAT: tetrakis dimethyl amino titanium

Figure 1. Schematic representation of the Ti precursors utilized for the synthesis of the N-TiO₂ thin films by plasma deposition.

high concentration of Ti-N species induces a red shift in the absorption gap of the material. Meanwhile Ti-NO species do not significantly modify the magnitude of the gap between the valence and conduction bands, but induce the formation of new localized states in the band gap zone of the oxide.

Finally, all these experimental and theoretical results are critically discussed in relation with the actual photoactivity of N-TiO₂ materials by analyzing the superhydrophilic conversion of the surface state of the prepared films under visible light irradiation.

2. Experimental Section

2.1. Thin Film Preparation. TiO₂ and N-TiO₂ thin films have been prepared by PECVD in a plasma reactor with a remote configuration. The system, supplied with a microwave plasma source (SLAN, from Plasma Consult, GMBh, Germany) has been described in previous works.^{27,28,35} It consists of an external 2.45 GHz microwave electron cyclotron resonance (MW-ECR) plasma source coupled to the reaction chamber and separated from it by a grid to avoid the microwave heating of the substrates. Under normal conditions of operation, the grid confines the plasma out of the reaction chamber (remote plasma conditions) where the substrate and the precursor dispenser are located. Titanium tetra-isopropoxide (TTIP), tetrakis(diethyl-amido)titanium(IV) (TDEAT), and tetrakis(dimethylamido)titanium(IV) (TDMAT) were used as titanium precursors. In Figure 1 we show a schematic representation of the structure of these three precursors, showing that four direct Ti-N bonds exist in TDEAT and TDMAT. It is likely that some of them can be preserved during the plasma processing of the N-TiO₂ thin films.

The plasma source was operated with a power of 400 W with either pure O₂ or N₂+O₂ mixtures at different proportions of nitrogen from 0% to 97%. The synthesis of the films was carried out at either 298 or 523 K, although most reported data corresponds to this latter temperature. Controlled dosing of the precursors was achieved by placing them in a stainless steel recipient heated to 305 K, while oxygen or a N₂/O₂ mixture was bubbled through it. Both the bubbling line and the shower-type dispenser used to dose the precursor into the chamber were heated to 373 K to prevent any condensation in the tube walls. The total pressure during deposition was 4×10^{-3} Torr (normal operation conditions). A deposition rate of approximately 2.5 nm min⁻¹ was estimated by means of a quartz crystal monitor for the samples grown at room temperature.

The different plasmas used for deposition of the films were characterized by optical emission spectroscopy (OES). The emission spectrum was analyzed using a 0.5 m CVI/Digikrom DK480 monochromator (CVI Laser Corporation, Albuquerque, NM) with a 1200 grooves/mm grating, spectra resolution of 0.2

nm, and spectral sensitivity ranging from 200 to 900 nm (Hamamatsu R928). The light is collected by a fiber optic, which is fixed to the monochromator and positioned 4 cm downstream from the source center. The light was collected through a hole in the air cooling ring. It should be noted that the spectroscopic intensities are integrated over the line of sight, thus limiting the spatial resolution.

All the films were deposited simultaneously on a silicon wafer and on quartz plates. The thickness of the prepared samples was estimated by measuring the mass thickness of the films by X-ray fluorescence (XRF) and Rutherford back scattering (RBS) or directly from cross section views in the electron microscope (note that for a given sample these two values do not coincide except for completely compact thin films). Most experiments were carried out with films with a thickness of some hundreds of nanometers.

2.2. Methods of Characterization. The optical properties of the samples were primarily determined by UV–vis absorption spectroscopy (Perkin-Elmer Lambda 12 Spectrometer) for samples prepared on fused silica. The ellipsometric characterization of the N–TiO₂ films was carried out in a J.A. Woollam VASE (variable angle spectroscopic ellipsometry) spectroscopic ellipsometer. Values of Ψ and Δ were obtained over the spectral range comprised between 300 and 1000 nm, at 5 nm resolution. To check the consistency of the data, they were collected at three angles of incidence: 65°, 70°, and 75°. Optical modeling and parameters fitting were carried out with the WASE32 program (J.A. Woollam Co., Inc.). To model the ellipsometric spectra, we fixed the thickness (thickness values were obtained by transversal scanning electron spectroscopy (SEM) images) and applied nonideal model options such as film thickness nonuniformity and angular spread of the beam entering the detector. Some fitting parameters were coupled among them, and their range was limited within defined values. Nonpartial polarization or monochromator bandwidth effects were considered. Quality assessment of the fit data was performed by using the mean-squared error (MSE) value. A small MSE implies that the assumed model was appropriate. In our case, the MSE was below 5 units in the absorbing region and below 2 units in the transparent region. The used optical model consists of two layers deposited on the Si (1 mm) substrate: an external region and an effective medium approximation (EMA) layer with a harmonic oscillator. In this layer, a Cauchy dispersion (with Urbach absorption) and a classic harmonic oscillator model were implemented in a single material layer. The Cauchy dispersion equation was used in the transparent region ($\lambda > 700$ nm). No dispersion of refractive index and the extinction coefficient was considered for $700 < \lambda < 1000$ nm. For $\lambda < 700$ nm, one or two harmonic oscillators were added to the Urbach absorption of the Cauchy model. Finally, a certain surface roughness consisting of 50% film material and 50% voids was assumed to describe the external layer.

X-ray photoelectron spectroscopy (XPS) spectra of the films were recorded on an ESCALAB 210 spectrometer working under energy transmission constant conditions. The Mg K α line was used for excitation of the spectra. They were calibrated in binding energy (BE) by referencing the different peaks to the C1s signal due to contamination taken at 284.6 eV. Quantification was done by calculating the area of the peaks and by correcting them with the sensitivity factor of each element/electronic level. To check the effect of surface impurities, the films were subjected to a gentle sputtering with Ar⁺ ions of 2.5 keV. A current density of about 10 $\mu\text{A cm}^{-2}$ for a sputtering time of 2 min was used for these treatments. No significant

changes in peak shape or in element ratio (except for the removal of most of the contaminating carbon) were found after this cleaning treatment. Fitting analysis of the N1s peak was carried out by using elemental bands of Gaussian/Lorentzian shape after background subtraction of the spectra with a Shirley-type curve.

SEM cross section and normal images were measured in a Hitachi S5200 field emission microscope for thin films grown on a silicon wafer.

Structural characterization of the thin films was done by X-ray diffraction in a Siemens D5000 diffractometer working in the Bragg–Brentano configuration and using the Cu K α line as excitation source.

Measurement of the surface electrical conductivity of the samples was carried out with the typical four-point probe test. A Keithley 617 Electrometer and a Hewlett-Packard 34401 A voltmeter were used for the measurements. These consisted of applying a voltage ranging between -0.25 and 0.25 V to the two external probes and the measurement of the current flowing between the two internal probes.

Measurement of water contact angles was carried out by the Young method by dosing small droplets of deionized and bidistilled water on the surface of the illuminated samples. In the experiments where the contact angle variation was determined as a function of the illumination time, a metal foil acting as a shutter was used to close and open the lamp output. All wetting angle measurements within a given experiment were taken after illumination for successive periods of time. Therefore, the time scale in the plots refers to the accumulative illumination of the samples. The maximum uncertainty in the determination of the water contact angle is about 10° depending on the sample position. In the course of this investigation it was noticed that the “as-prepared” thin films were more hydrophilic than the same samples some time after their preparation. Therefore, the reported results correspond to samples that were stored in desiccators for at least 2 months before testing their photoactivity. Illumination of the samples was carried out with a Xe discharge lamp with photon intensity at the position of the samples of 2 W cm^{-2} for the complete spectrum. For simplicity we will refer to this situation in the text and figures as UV illumination. Other experiments consisted of the illumination with the same lamp by placing a UV filter (i.e., $\lambda > 400$ nm) between the lamp and the sample. The light intensity at the sample position was then 1.6 W cm^{-2} . In all cases, an infrared filter (i.e., a water bath) was kept between the lamp and the samples to prevent any possible heating by the infrared radiation.

2.3. Computational Details. All the calculations were performed using the Vienna Ab-initio Simulation Package (VASP) 4.6 code.^{36–38} Instead of using a GGA method,^{39,40} we decided to use LDA+U, since, as will be explained below, there are some studies which confirm its validity to study the electronic structure of this system. Inner core electrons were described by the projector-augmented-wave (PAW) method⁴¹ and a 500 eV cutoff energy. The Ti (3s, 3p, 3d, 4s), O (2s, 2p), and N (2s, 2p) electrons were treated as valence states, while the remaining electrons were kept frozen as core states. The optimization of the structures was performed via a conjugated gradient technique, which utilizes the total energy and the Hellmann–Feynman forces on the atoms (and stresses on the unit cell). The Brillouin-zone integrations were performed using Monkhorst–Pack grids,⁴² using a $(2 \times 2 \times 1)$ mesh, with which convergence in energy was achieved. The simulation cell is formed by a $2 \times 2 \times 3$ repetition of the anatase unit cell, in which there are 72 Ti atoms and 144 O atoms. We employed a

LDA+U approach, as described by Dudarev et al.,^{43–45} with a value of U of 4.5 eV. Calzado et al.⁴⁶ found that this value of U yields a correct description of the gap states in periodic LDA+U calculations. All calculations were carried out in the Finis Terrae supercomputer, in Santiago de Compostela, Spain.

3. Results

3.1. State and Concentration of Nitrogen in N-TiO₂ Thin Films. The amount of nitrogen incorporated in the film varied by changing the precursor and the plasma process parameters. Adjusting the plasma gas composition by using different O₂+N₂ mixtures as plasma gas was very important for this purpose. The OES spectra of the plasmas of these mixtures for N₂ concentrations higher than 80% were characterized by a series of peaks and bands attributed to N₂* and N₂⁺ species (see Supporting Information S1).^{47,48} These nitrogen bands substitute those attributed to O₂* and O* that characterize the spectra recorded in our experimental system when pure oxygen is used as plasma gas.²⁷ A summary of the main species and spectral features detected as a function of the O₂/N₂ ratio are reported in the Supporting Information S1 and in a previous contributions.⁴⁹ From this analysis it is important to realize that, although nitrogen excited species detected by OES are the majority in the N₂/O₂ plasmas, this does not necessarily preclude the formation of activated oxygen species, but just indicates that the average lifetime of these latter species is short as compared with that of the nitrogen species. The high reactivity of the oxygen species accounts for the formation of a titanium oxide film and enables the release of the carbon and hydrogen atoms of the precursors in the form of volatile oxidized compounds. Simultaneously, the presence of active species of nitrogen in the plasma provides a mechanism for the incorporation of nitrogen in the film by the reaction with the partially decomposed precursor molecules in the plasma phase or on the surface of the growing film. We will show later that the amount and type of incorporated nitrogen depends on the ratio between nitrogen and oxygen in the plasma gas.

Plasma deposition of TiO₂ thin films has typically been carried out by using TTIP as the titanium precursor. The use of other precursors such as TDMAT and TDEAT offers the possibility to incorporate some nitrogen within the structure, even if no molecular nitrogen is added to the plasma gas, provided that some of the Ti–N bonds existing in the precursor molecules are preserved in the films. To verify this possibility we have analyzed by XPS a series of films prepared with a plasma of pure oxygen but using TTIP, TDMAT, and TDEAT as precursors and 523 and 298 K as substrate temperatures. It was found that small amounts of nitrogen became incorporated in the films prepared with TDMAT and TDEAT precursors (see Supporting Information S2). The incorporation was more favorable at 298 K. For all samples, the O1s and Ti2p spectra were similar to those amply reported in the literature for TiO₂.⁵⁰ The N/Ti ratios deduced from the quantitative analysis of the spectra of the N-TiO₂ films prepared at 523 K and O₂ as the sole plasma gas were 0.037, 0.017, and 0.0 for the TDEAT, TDMAT, and the TTIP precursors, respectively. The N1s spectra of the two former films were characterized by a broad peak at around 400 eV (see Supporting Information S2), which is commonly attributed to interstitial nitrogen species bonded to titanium and oxygen (i.e., a kind of Ti–N–O species^{12,22}). Similar spectra were obtained when the deposition was carried out with a substrate temperature of 298 K, although the intensity of the N1s signal was approximately twice higher in this case. It is also important to mention that the width of this N1s peak was also higher at 523

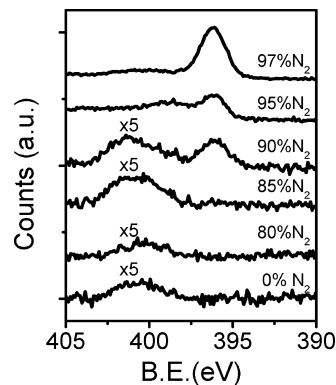


Figure 2. N1s spectra recorded for a series of N-TiO₂ thin films prepared with the TDMAT precursor and different percentages of N₂ in the plasma as indicated. Note that some spectra are affected by a multiplication factor to bring them into a common scale.

K (i.e., a half width at half-maximum (HWHM) of 2.8 eV) than at 298 K (i.e., a HWHM of 1.8 eV). This difference suggests that the nitrogen signal at 523 K is a convolution of different species of nitrogen. N1s spectra with more than one component at around 400 eV have been reported by several authors.^{51–53} Their development in our case would indicate that at 523 K there are nitrogen species with slightly different geometries and bonding arrangements.

The concentration and type of nitrogen species in the N-TiO₂ thin films changed when O₂+N₂ mixtures were used as plasma gas. Under these conditions the main parameter controlling the incorporation of nitrogen into the films was the concentration of nitrogen in the gas mixture. Figure 2 shows a series of N1s spectra taken for films prepared at 523 K by using TDMAT as the titanium precursor and increasing concentrations of N₂ in the plasma gas. Similar spectra were obtained for the other precursors. It is found that for percentages of N₂ higher than 85%, a new nitrogen species at around 396 eV appears in the spectrum. This species becomes dominant for higher percentages of nitrogen in the plasma gas. Similar results were obtained for the two other precursors, thus sustaining that the plasma gas composition and not the type of precursor is the main variable controlling the amount of nitrogen incorporated into these films. This new form of nitrogen has been attributed on the basis of XPS studies of nitride species in substitutional positions of the titanium oxide lattice (i.e., a Ti–N species^{1,7,10,53–55}). The combined XPS, near-edge X-ray absorption fine structure (NEXAFS), and Rietveld analysis made recently by Chen et al.⁵⁵ for ammonia-treated titania have quite unequivocally supported this attribution. It is also worthy of note that for most investigated films the shape of the O1s and Ti2p spectra is similar to that reported for TiO₂, thus indicating that the upmost surface layers of the films have become oxidized by exposure to the air. Nevertheless, the shape of the Ti2p spectrum of the films prepared with a 97% of nitrogen in the plasma gas slightly changed with the development of a shoulder at lower BE, evidencing that some Tiⁿ⁺ species ($n < 4$) remain in the surface of this sample even after its handling in air.

A deeper insight into these spectra can be obtained by fitting. Figure 3 shows such an analysis for some selected case examples taken from Figure 2 and others corresponding to thin films prepared with TTIP as precursor. The two sets of samples were synthesized with relative N₂ contents in the plasma gas of 0, 90, and 97%. In the case of the TDMAT samples, the spectra can be properly fitted with four bands located at 396.1, 399.3, 400.7, and 401.7 eV, the three latter accounting for the broad

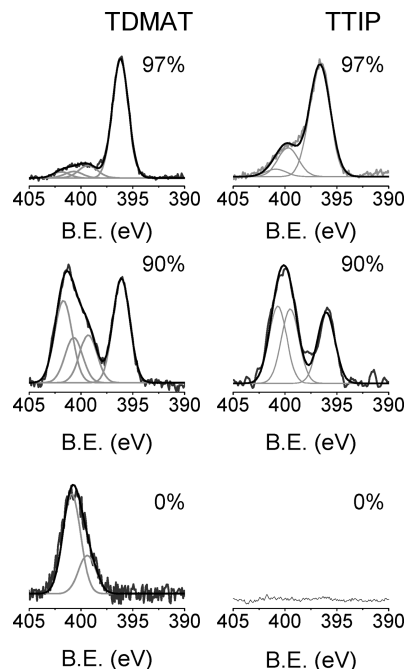


Figure 3. Fitted (gray line) and experimental (black line) N1s normalized spectra of selected N–TiO₂ thin films prepared at 523 K with the TDMAT (left) and the TTIP (right) precursors and different percentages of N₂ in the plasma gas. Elemental bands used for fitting are plotted in gray.

peak at around 400 eV. Meanwhile, a reasonable fitting could be obtained for the spectra of the TTIP samples by using just three bands at 396.1, 399.3, and 400.7 eV. A variety of peaks with N1s BEs comprised between 399 and 402 eV were already found in the early work of Saha et al.⁵⁶ dealing with the thermal oxidation of titanium nitride. Because of the similarities of the preparation techniques, it is also worth mentioning a recent publication by Chen et al.²⁶ where they investigated by XPS the type of nitrogen species incorporated into N–TiO₂ powder samples prepared by an atmospheric plasma procedure and posterior annealing. These authors found different components in the N1s photoelectron spectra, which they attributed to Ti–N (395.8–397.8 eV), Ti–NO (398.8–401.2 eV), and Ti–NO₂ (402.0–403.0 eV) species, in good agreement with our own results. Another relevant result of that work was the verification that the latter species was inactive in inducing any visible photocatalytic activity. Similarly, Dunnill et al.,⁵⁷ using a thermal chemical vapor deposition process at 500 °C for the preparation of N–TiO₂ thin films, found that in the majority of cases a peak at 400 eV was the only species detected and that these samples presented photocatalytic activity in the visible. On the basis of these and many other recent studies,^{1,7,10,12,22,51–55} we attribute the different features to Ti–N (i.e., band at 396.3 eV assigned to nitrogen triple bonded to titanium) and to nitrogen in a titanium oxinitride local environment (399.3 and 400.7 eV), where nitrogen simultaneously bonds to oxygen and to titanium in a defective lattice site (i.e., in a kind of Ti–N–O or Ti–O–N local structure). Meanwhile, the fourth band at 401.7 eV, observed in samples prepared with the TDMAT and TDEAT precursors, must be attributed to N bonded to a less electro-positive environment or, alternatively, to a large number of oxygen atoms. Therefore, we tentatively attribute this band to Ti–NO₂ species (i.e., a nitrogen atom bonding simultaneously to one titanium and two oxide ions of the lattice²⁶). A similar attribution has been made recently by Asahi et al.⁵³ based on first principles calculations for a peak with a BE higher than

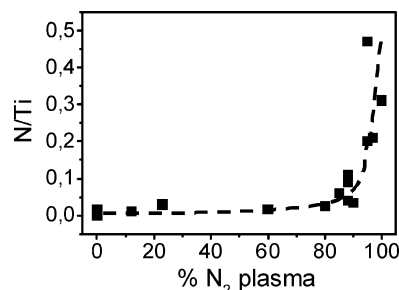


Figure 4. N/Ti ratio determined from the intensities of the N1s and Ti2p photoelectron peaks as a function of the percentage of nitrogen in the O₂+N₂ mixture used as plasma gas. The dashed line is included to guide the eyes.

that of the band used here for fitting. For simplicity, in the rest of the paper we will refer to Ti–N and Ti–NO species (the latter including the species that we have designed as Ti–ON), even if different environments, and therefore BEs, can be expected for the different interstitial species of nitrogen. Theoretical calculations have been performed for Ti–N (i.e., N_s according to the notation used by the model systems' calculations Ti–NO (i.e., N_i) and Ti–ON (i.e., N_{si}) species in section 3.3.

XPS has been also used to quantitatively estimate the concentration of nitrogen in the films as a function of the plasma deposition conditions. Figure 4 shows a plot of the N/Ti ratio as a function of the relative concentration of nitrogen in the plasma gas determined by XPS for an ample series of thin films prepared at 523 K. In this plot we make no distinction according to the precursor used for their synthesis, as the plasma gas composition is the main parameter controlling the nitrogen content. It is also important to mention that at 298 K the amount of incorporated nitrogen was always slightly higher than that at 523 K for N₂/O₂ ratios higher than 50% (data not shown). The plot in Figure 4 shows that the concentration of nitrogen in the film remains relatively constant up to N₂ percentages of 80–85%. Above these values, the concentration of nitrogen in the films sharply increases, reaching N/Ti ratios of ca. 0.5 when a 97% nitrogen plasma was used for the synthesis. As mentioned previously, for this sample the shape of the Ti2p spectrum broadens toward lower BEs, pointing to certain reduction of the titanium cations and the formation of oxygen vacancies within the lattice. The incorporation of nitrogen, particularly in the form of Ti–N species, and its relationship with the formation/elimination of oxide vacancies within the lattice has been addressed previously in the literature both experimentally and theoretically.^{25,34,54,55} In relation with these previous works dealing with an already formed TiO₂ network where nitrogen is added either by ion implantation or upon annealing in ammonia, our experimental conditions are different because the N–TiO₂ materials are created directly by the deposition and/or reaction of/with plasma species. However, the fact that the maximum concentration of Ti–N species appears when the oxide is defective suggests that the incorporation of this nitrogen species becomes favored in partially reduced titanium oxide networks.

3.2. Optical and Electrical Properties of N-Doped Titanium Oxide Films. The progressive incorporation of nitrogen into the films, particularly in the form of Ti–N species, induces significant changes in their optical behavior. Figure 5 shows a series of UV–vis absorption spectra recorded for selected thin films prepared with TDMAT as precursor and 85%, 90%, 95% and 97% N₂ in the plasma gas. It is important to note that the three latter samples, have incorporated a considerable amount

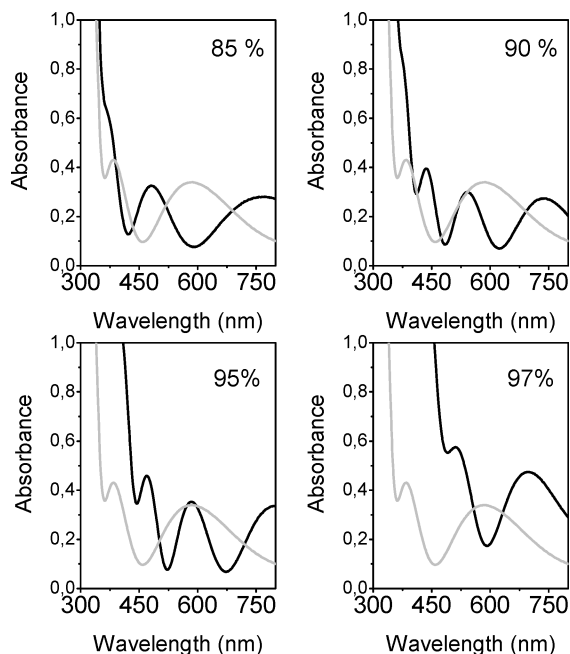


Figure 5. Set of absorption spectra recorded for a series of N–TiO₂ thin films prepared at 523 K with the TDMAT precursor and different percentages of nitrogen in the plasma gas as indicated in each particular panel. The gray spectrum included for comparison in each panel corresponds to the absorption spectrum of a pure TiO₂ thin film.

of nitrogen (cf. Figures 3 and 4). These spectra are compared with the spectrum of a film prepared with 0% N₂ taken as a reference. All the curves are characterized by the typical oscillatory behavior found when a high refractive index (**n**) material is deposited on a transparent substrate with smaller **n**. These oscillations are originated by the interference of the partially reflected beams at the film/air and film/substrate interfaces.⁵⁸ Besides these oscillations, another quite remarkable effect is the shift of the absorption threshold to lower wavelengths for thin films prepared with percentages of nitrogen higher than 85%. Usually, this shift has been recognized in the literature as a hint of visible photoactivity in doped TiO₂,^{17–20} although this correlation has been claimed as a necessary but not sufficient condition.^{22–24,59} It is also important to remark in this figure that the minima of the oscillations recorded for the sample prepared with 97% N₂ appear quite above the curve of the reference TiO₂, which indicates a significant absorption in the visible region (i.e., for $\lambda > 500$ nm). For percentages of N₂ in the plasma smaller than 85%, for which the amount of incorporated nitrogen is still small (c.f. Figures 3 and 4), the shape of the curves, except for the oscillatory behavior in the transparent region that depends on the film thickness, was similar to that corresponding to the film prepared with 0% N₂ and did not depict any clear hint of a shifted absorption edge. Similar sets of curves were obtained when using either TTIP or TDEAT as the titanium precursor. For the whole set of investigated samples, we have calculated the value of the absorption threshold by assuming a Tauc model for the evaluation of the band gap of TiO₂ (i.e., $A(h\nu)^{1/2}$).⁶⁰ The obtained values are represented in Figure 6. The shape of the curve defined by the different points is the reverse of that in Figure 5, this latter corresponding to the relative concentration of nitrogen incorporated into the films. Consequently, a representation of the absorption threshold values against the N/Ti ratio in the films follows a linear tendency (see Supporting Information S3). This behavior indicates that the absorption threshold of the N–TiO₂ films is controlled by the amount and perhaps the type of

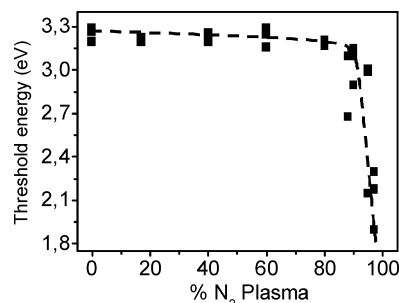


Figure 6. Values of the absorption threshold plotted against the percentage of nitrogen in the plasma gas for N–TiO₂ thin films prepared with the TTIP, TDMAT, and TDMAT precursors at 523 K. The dashed line is included to guide the eyes.

incorporated nitrogen. For the samples prepared with N₂ percentages higher than 85%, the Ti–N species is the most abundant species, as evidenced by the shape of the XPS spectra in Figures 2 and 3. These samples present a clear shift in the absorption threshold whose magnitude is correlated with the amount of nitrogen within the lattice (cf. Figures 5 and 6). By contrast, samples prepared with 85% or a lesser amount of nitrogen in the plasma, incorporate a limited amount of nitrogen in the form of Ti–NO species. These samples do not present a clear shift in the absorption threshold, although a clear determination is difficult with absorption spectra such as those in Figure 5, where the presence of interference oscillations may mask changes at the edge spectral region.

Electrical characterization of the films prepared with a high concentration of N₂ in the plasma gas showed that they present a certain sheet conductivity (see Supporting Information S4), which is indicative of some reduction of the titanium ions and the presence of a certain concentration of oxygen vacancies within the lattice.⁶¹ The broad absorption feature extending through all the visible region of the spectra (i.e., $\lambda > 500$ nm) found for the samples prepared with 97% N₂ can therefore be associated with the lost of stoichiometry in these samples.²¹ This confirms our evidence based on the analysis of the Ti2p XPS spectra and supports the already mentioned relationship between the incorporation of Ti–N species and the formation of oxygen vacancies within the lattice.^{25,34,54,55}

Owing to the oscillatory behavior of the UV–vis transmission spectra, it is difficult to ascertain whether real absorption features close to the absorption threshold superimpose in the spectra of the films prepared with percentages of N₂ lower or equal than 85%, where only Ti–NO species have been determined by XPS. In order to check this point, we employed ellipsometry to determine the extinction coefficient (**k**) and refractive index (**n**) functions of selected films for $\lambda > 300$ nm. The corresponding plots are shown in Figure 7 for three thin films prepared at 523 K with TDMAT as the precursor and percentages of N₂ in the plasma gas of 0%, 85%, and 97%. For the whole spectral region, the refractive indices of the 97% N₂ film was higher than those of the other two samples (e.g., at $\lambda = 550$ nm, the measured values were 2.38 and 2.12, respectively), in agreement with its UV–vis absorption spectrum (Figure 5) and its extinction coefficient curve plotted in the bottom panel of Figure 6. This latter curve is characterized by a broad and intense maximum at around 400 nm that defines a shifted absorption threshold of 2.11 eV, extending through the whole visible region of the spectrum. By contrast, the extinction coefficient curve of the film prepared with 85% nitrogen does not present this broad absorption and its edge jump defines an absorption threshold of 3.19 eV, quite similar to that of the film prepared with pure

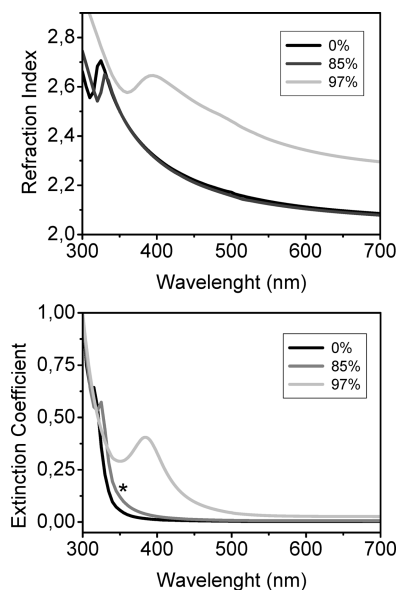


Figure 7. (Top) Refraction index and (bottom) extinction coefficient curves determined for N-TiO₂ thin films prepared at 523 K by using TDMAT as a precursor and different percentages of N₂ in the mixture used as plasma gas as indicated. The star points to the region whose reproduction is only possible by admitting an oscillator around 375 nm.

oxygen as plasma gas. The main difference between the curves of the samples prepared with 0% and 85% N₂ consists of a small but well-defined absorption feature at around 375 nm in the extinction coefficient curve of the latter (indicated by a star in the figure). An absorption feature in this position was indeed needed to extract a reasonable extinction coefficient curve from the ellipsometric data recorded for this film.

3.3. DOS Calculations for Model N-TiO₂ Systems. The three model systems used to calculate the DOS of the different N-TiO₂ thin films are shown in Figure 8. They represent the substitutional, N_s, interstitial, N_i, and substitutional–interstitial, N_{si}, defect states. In this latter type of defect state, N occupies the same position as in the case of the N_s defect, but there is also an O atom occupying an interstitial site. We will assume that these states of nitrogen correspond to the XPS bands identified in section 3.1 and attributed to Ti–N, Ti–NO, and Ti–ON species. Calculations based on structures similar to those of the two former types of defects have been previously carried out by Di Valentin et al.^{12,13,15} to account for modifications of

TABLE 1: Relevant Distances (in Å) Involved in the Three Types of Defects Studied: N_i, N_s, and N_{si}^a

species	O–Ti	N–O	N–Ti
N _i –C	2.06, 2.06, 2.01	1.48	1.95, 1.98, 2.05
N _i –S	2.13, 2.13, 2.28	1.36	2.06, 2.06, 2.28
N _s –C			1.98, 2.00, 2.07
N _s –S			2.00, 2.00, 2.09
N _{si} –C	2.09, 2.17, 3.33	1.29	1.98, 2.02, 2.04
N _{si} –S	2.17, 2.17, 3.30	1.28	2.02, 2.03, 2.03

^a The distance between the two defects in the unit cell is taken into account by labeling with C and S the structures in which the N atoms are close and separated, respectively.

the band structure in N-doped TiO₂. These authors have also considered either the effect of Ti–N^{12,13,15} or Ti–NO-like^{12,13} species, although they employed smaller simulation cells (with 96 and 72 atoms for the anatase and rutile supercells, respectively). Herein, besides studying the effect of another type of species (i.e., Ti–ON), we systematically address the possible influence in the electronic structure of the concentration of incorporated nitrogen for both the Ti–N and Ti–NO species in a larger supercell with 216 atoms. To simulate the influence of the concentration of nitrogen in real samples, we have considered two different simulation cells for each system, one containing one defect, and another containing two defects. In addition, in this latter case we have used two different arrangements for the two defect states, placing them in either two nearby or in quite separated positions within the lattice. These two geometries are employed to represent the electronic structure of N-TiO₂ systems with, respectively, a high and a low concentration of nitrogen. The most relevant geometrical parameters of the studied defect configurations are reported in Table 1.

We also performed calculations on a different type of defect, in which the O atom was initially placed at its equilibrium lattice location, and the N atom is in an interstitial site above the O atom at a distance of 1.35 Å along the *z* axis. We studied two systems with one and two defects of this kind. Upon energy minimization, the cells underwent large geometrical rearrangements, leading in the two cases to final configurations equivalent to that of the N_i defects. This suggests that this initial configuration is not stable and that minimization of the energy is accomplished by a displacement of the O atoms from their initial location and their substitution by nitrogen. This also means that the assumed detection by XPS of these species in some of our samples (i.e., band at 401.7 eV of BE, cf. Figure

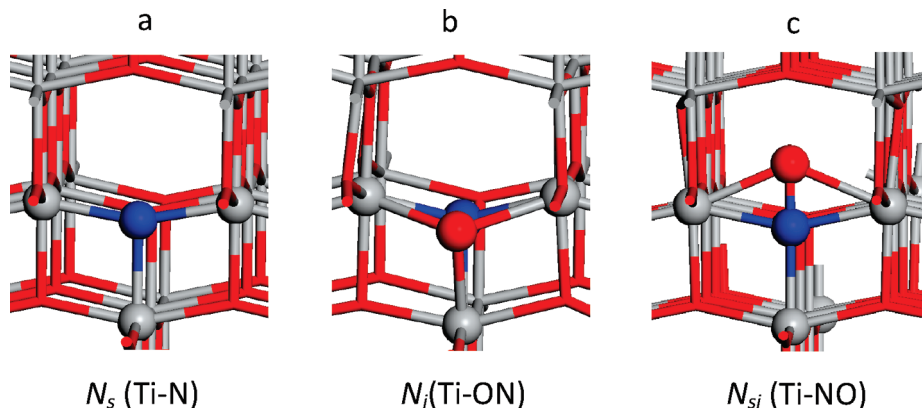


Figure 8. Structures of the three types of N centers studied. (a) Substitutional defect, N_s, in which a N atom replaces an O atom. (b) Interstitial defect, N_i, in which the N atom is located in an interstitial place, and the O atom is also displaced from its original site. (c) Substitutional–interstitial defect, N_{si}, in which the N atom occupies the same position as in the case of the N_s defect, and the O atom occupies an interstitial place.

3) is likely related to the fact that the plasma deposition process utilized for the synthesis of the N–TiO₂ films is an out-of-equilibrium procedure.

The calculations also provided interesting information regarding the energy of the different studied systems. Thus, when TiO₂ is modified with N_s defects, the energy of the system where the two defect states are in nearby positions is 29.1 kJ/mol higher than the energy of the system in which the two defects are far away. When considering N_i defects, this energy difference is much smaller, just −1.1 kJ/mol, which means that there is no strong energetic driving force preventing the aggregation of N_i defects. In the case of N_{si} defects, this energy difference is 14.0 kJ/mol, indicating that it is energetically favorable to keep N_{si} defects as far away as possible within the lattice. On the other hand, to determine the relative stability of the N_{si} and N_i defect states, we can directly compare the energies of the corresponding systems, as they have the same number of atoms. For the systems modeling low nitrogen concentrations (with defects far away from each other), we find that N_i defects are 8.3 kJ/mol more stable than N_{si} defects. Meanwhile, for the systems modeling a high concentration of nitrogen, the N_i defects are 29.0 kJ/mol more stable than N_{si} defects, a result that suggests that TiO₂ materials with a high concentration of nitrogen will tend to have N_s and N_i defects and that the formation of N_{si} defects would not be favored.

The total DOS calculations for pure TiO₂ (shown in the Supporting Information S6) predict a gap between the valence and conduction bands of 2.7 eV. This value is smaller than the experimental band gap of anatase TiO₂ (i.e., 3.2 eV⁶²), a difference that is due to the well-known underestimation of the band gap in DFT calculations.⁶³ The value of the Hubbard parameter *U* that we used is 4.5 eV, which provides a good description of the gap states in periodic LDA+*U* calculations of TiO₂ and, at the same time, predicts a reasonably good value for the band gap (i.e., 2.7 eV).⁴⁶ A similar result was also obtained by Di Valentin et al.¹¹ when modeling N–TiO₂ systems.

The total DOS of the six studied N–TiO₂ systems are shown in Figure 9. The reported results indicate that the N–TiO₂ systems have developed new electronic states in the band gap close to the valence states of titanium dioxide. A similar result has been obtained by other authors simulating the electronic structure of N–TiO₂ systems,^{11–15,25,34} although in these previous works smaller supercells were employed in the calculations. Particularly interesting with regard to the optical properties of N–TiO₂ is the difference observed in Figure 9 between the shape of the gap states corresponding to the N_s and the N_i and N_{si} defects around the highest occupied molecular orbital (HOMO) level (marked with a solid line in the figure). In the former case (i.e., DOS curves a and b), the extra states due to the incorporation of N appear as a continuous prolongation of the valence band states of pure TiO₂ (marked with a dashed line in the figure). By contrast, for the case of N_i and N_{si} defect states, the N-related gap states appear as well-defined discrete peaks separated from the valence band of TiO₂ (i.e., DOS curves c–f). Phenomenologically, this difference is equivalent to saying that the N_s defects have induced a shift of the valence band edge and produced, a decrease in the gap of the system, while the N_s and N_{si} states do not modify the valence band of TiO₂ but introduce new electronic states in the gap. This point has been previously discussed on the basis of both experimental⁵⁴ and theoretical^{11–15} studies. Thus, Diebold et al.⁵⁴ studied by XPS and valence band photoemission N-implanted anatase and rutile, and concluded that localized states rather than a band

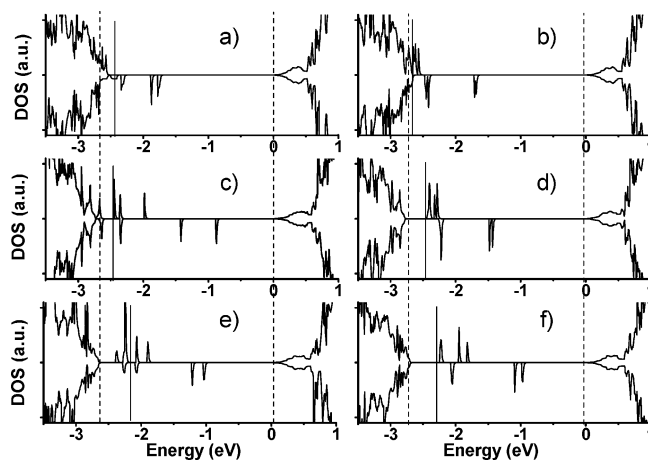


Figure 9. DOS plots of the six N–TiO₂ systems studied, showing the two spin components separately. Plots a and b correspond to the two systems with substitutional N doping (N_s), with two N atoms located at close and separated positions, respectively. Plots c and d correspond to the two systems with interstitial N doping (N_i), with two N atoms located at close and separated positions, respectively. Plots e and f correspond to the two substitutional–interstitial N configurations (N_{si}), with two N atoms located at close and separated positions, respectively. The bands are plotted in such a way that the origin of the energy (0 eV) is placed at the bottom of the conduction band. The two vertical dashed lines are placed to indicate the HOMO–LUMO (lowest unoccupied molecular orbital) gap in TiO₂. The vertical solid line indicates the highest occupied orbital of the system, which in the case of N–TiO₂ corresponds to new gap states generated by the presence of nitrogen in the lattice.

gap narrowing develop upon nitrogen implantation and the subsequent formation of N^{3−} (i.e., Ti–N) species. Theoretically, studying the anatase polymorph, Di Valentin et al.^{11,12} concluded that substitutional nitrogen states (i.e., Ti–N) lie just above the valence band, while interstitial nitrogen states (i.e., Ti–NO) lie higher in the gap. These authors also found that Ti–N species in rutile might produce a certain increase of the gap with the N-associated states close to the valence band maximum.¹⁵ The main difference between these previous studies and our calculations reside in the fact that we deal with more than one nitrogen species and define two different scenarios for them, depending on whether they are located in separated or close positions of the lattice. When N atoms are close, as in the DOS curves a, c, and e, the number of gap states is higher and appear more scattered along the band gap, as if there is a splitting of peaks due to the electronic interaction between defects. By contrast, when the N atoms are separated within the lattice, as in DOS curves b, d, and f, there is a smaller number of peaks in the gap, and they tend to be more concentrated around certain energy values in the band gap (i.e., more localized states). In particular, for the N_s species located in nearby lattice positions, it appears that the TiO₂ valence band maximum extends continuously to higher energies. From an experimental point of view, this is equivalent to saying that there has been a narrowing of the gap. This would be in fact the situation for our samples prepared with nitrogen percentages in the plasma higher than 85% (cf. Figures 4 and 5).

As shown in the partial DOS plots in Figure 10, the new states developed in the gap have a mixed titanium–nitrogen–oxygen character and show slightly different features depending on the kind of nitrogen defect considered in each case. This figure represents in an enlarged scale the gap zone to clearly depict the new states appearing in the N–TiO₂ systems. The plots represent the titanium, oxygen, and nitrogen projected states of the DOS curves in the regions around the HOMO lines

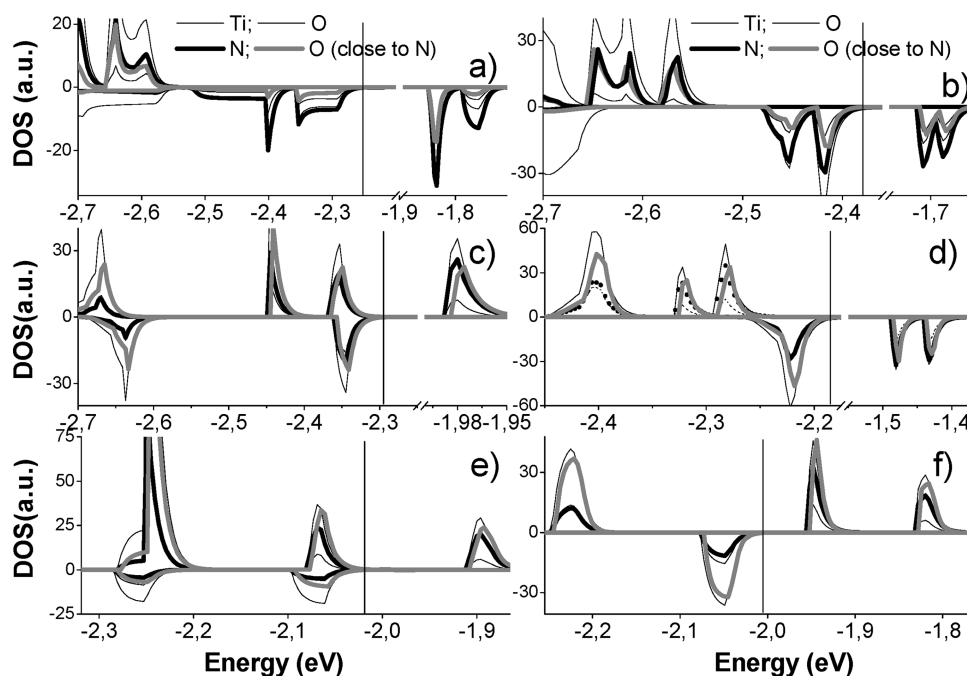


Figure 10. Partial DOS plots of N, Ti, and O in the gap states for the six studied N-TiO₂ systems with the labeling a-f being the same as that in Figure 9. The oxygen contribution is differentiated for the oxygen atoms close to the nitrogen and the rest of oxygen atoms of the lattice. The total DOSs plotted in Figure 9 are calculated as the sum of these partial DOSs. The vertical solid line indicates the highest occupied orbital of the system.

in each system (note that the HOMO lines appear at different energies in each case). For oxygen, they represent both the states corresponding to the oxygen atoms close to nitrogen and those located in separated positions. This distinction is important since for the N_i and N_{si} states, nitrogen is directly bonded to an oxygen atom whose contribution to the DOS of the new states is expected to be quite substantial. The first conclusion we could draw from these plots is that all the defect states have a mixed character with contributions from the oxygen, nitrogen, and titanium atoms. However, a closer look at these curves also reveals that in the N_s defects the nitrogen contribution to the gap states is relatively higher than that of the close oxygen atoms, while for the N_i and N_{si} defects the nitrogen and close-oxygen contributions are rather similar, thus supporting the importance of these oxygen atoms in determining the electronic properties of the system. This closer look to the new states around the HOMO line also suggests that the DOS curves of the N_s defects, particularly for the case with the two nitrogen atoms located in nearby positions, are a continuous extension of the valence band. The fact that the nitrogen contribution to these states extends through the entire DOS region, both below and above the HOMO line, supports our view in the sense that a narrowing of the valence band has occurred in this case. By contrast, for the N_i and N_{si} defects, the nitrogen contribution to the new states appears quite concentrated in localized levels that do not form a continuum with the valence band states. This result suggests that even for N-TiO₂ systems with a high concentration of Ti-NO species, their electronic structure can be described by the appearance of localized states in the gap.

3.4. Wetting Angle Photoactivity of N-TiO₂ Thin Films.

The photoactivity of N-TiO₂ thin films has been the subject of a large debate during past years.¹⁻¹⁴ In recent publications we have shown that transformation of the surface state of N-TiO₂ from partially hydrophobic (i.e., wetting contact angles around 80°) into hydrophilic can be induced by visible light in samples containing Ti-NO species, regardless of whether they were amorphous or crystalline. By contrast, visible photocatalytic

activity toward, for example, the photodegradation of dyes seems a more demanding process which requires titanium oxide to be in crystalline phase, forming a mixture composed mainly by anatase and a small amount of rutile.²²

In agreement with previous studies with PECVD TiO₂ thin films using TTIP as a volatile precursor of titanium and pure oxygen as plasma gas²⁵, we have found that amorphous TiO₂ is obtained for deposition temperatures lower than 523 K and that the anatase phase of this oxide is obtained for $T \geq 523$ K. By contrast, most N-TiO₂ thin films prepared at this temperature with TDMAT and TDEAT as precursors were amorphous, as shown by their XRD spectra (see Supporting Information S7). Since no photocatalytic activity was found for any of the N-TiO₂ thin films when illuminated with visible light and very little when using UV light, to check the possible role of the different nitrogen species in controlling the visible photoactivity of these materials we have looked for changes in wetting contact angle under visible and UV light illumination. Figure 11 presents some selected results showing that for samples containing Ti-NO species (i.e., a sample prepared with 85% N₂) the wetting angle decreases by almost 50° when illuminated with visible light, while for the films with a high concentration of Ti-N species (i.e., sample prepared with 97% N₂) no visible light effect was observed. This different behavior according to the type of nitrogen species was common for the rest of N-TiO₂ thin films. When after the visible illumination the samples were irradiated with UV light, we found that all of them became superhydrophilic (i.e., wetting angle lower than 10°), which is the typical behavior of UV-illuminated TiO₂ thin films. Even if wetting-induced changes and photocatalytic processes are not equivalent tests of TiO₂ photoactivity,^{22,64} the reported results in Figure 11 clearly prove that Ti-N species are unable to induce visible light photoactivity and that the presence of Ti-NO species in the films is a requisite for promoting visible light activation of N-TiO₂ thin films, at least for a partial hydrophilic conversion of their surface.

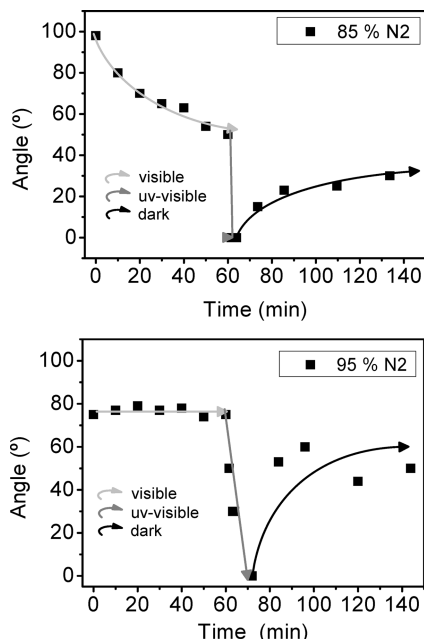


Figure 11. Evolution of the wetting angle as a function of the illumination time with visible and UV lights and then left in the dark for N-TiO₂ samples prepared with 85% (top) and 97% (bottom) of N₂ in the plasma gas. The lines are plotted to guide the eyes.

4. Discussion

The previous results on N-TiO₂ thin films prepared by PECVD have provided information about the influence of the incorporated nitrogen on both the optical properties of TiO₂ and the characteristics of the nitrogen species incorporated within the structure of the oxide according to the different conditions of preparation. In relation to this latter aspect, we have also described theoretically how the different species of nitrogen may affect the electronic structure of the prepared materials. The influence of these species of nitrogen on the photoactivity of N-TiO₂ is finally discussed in relation with the visible-light hydrophilic conversion of the surface of the prepared films.

4.1. Type and Concentration of Nitrogen Species and Band Gap Narrowing in N-TiO₂ Thin Films. The previous XPS results have shown that the incorporation of small amounts of nitrogen in the form of Ti-NO species (i.e., N_i defects according to the notation used for the DOS calculations) occurs when using TDMAT or TDEAT as precursors or when the films are deposited with a O₂+N₂ plasma mixture with less than 90% of nitrogen. We have proposed that the existence of four Ti-N bonds in the two latter precursor molecules may account for the presence of Ti-NO species in these films, even if no nitrogen gas has been added to the plasma. For 90% or higher concentration of nitrogen, a progressive incorporation of Ti-N species takes place. For all experimental conditions used for the synthesis of the N-TiO₂ films, we have also found that the amount of incorporated nitrogen species (Ti-N and Ti-NO) was higher at low (i.e., 298 K) than at high (523 K) temperatures. The stability of Ti-N implanted in rutile and anatase polymorphs of TiO₂ has been addressed in previous articles,^{34,54} where a certain desorption upon annealing has been observed only for the case of anatase⁵⁴ and an extra stabilization is achieved when gold is deposited onto the surface.³⁴ These results have been interpreted in terms of the interaction of the implanted nitrogen (and deposited gold particles) with oxygen vacancies in the lattice.^{25,34,54} Although most of our films were amorphous and a comparison with literature data is therefore not straight-

forward, we must stress that our results point to a certain relationship between the formation of Ti-N species and the existence of oxygen vacancies within the lattice. The aforementioned dependence of the Ti-N concentration on the temperature of the PECVD process and the fact that the maximum concentration of this species is found for defective and high conductive samples support such dependence.

Ti-N and Ti-NO species of nitrogen have been previously detected and discussed in literature,^{1,12,22,51–57} although no complete agreement exists on their specific role in altering the electronic and optical properties of N-TiO₂ materials. In fact, during the last years there has been a vivid discussion on whether modifying the TiO₂ with nitrogen produces a shift in the absorption edge or just the development of absorption centers close to an unmodified gap. Our experimental results indicate that both localized band states and band gap narrowing may occur depending on the type and concentration of nitrogen species incorporated within the films. Thus, we have experimentally found that the incorporation of a relatively low concentration of interstitial nitrogen (i.e., Ti-NO species) does not substantially modify the band gap structure of the oxide, but induces the formation of some localized electronic states in the gap (cf. Figures 5 and 7). A similar situation has been claimed in the theoretical works of Di Valentin et al.^{11–15} By contrast, our data suggest that a narrowing of the band gap due to a shift in the valence band edge may occur when substitutional nitrogen (i.e., Ti-N species) is incorporated within the lattice. We have also found that the magnitude of this shift is directly related with the amount of incorporated Ti-N species that we control by changing the relative amount of nitrogen in the plasma. In recent experimental⁵⁴ and theoretical^{11–15} studies on titanium oxide with incorporated Ti-N species, such a narrowing has not been detected, a difference that might be related with the fact that in these experiments a lower concentration of nitrogen species was actually incorporated within the lattice and because only the effect of isolated nitrogen species was theoretically modeled.

The films with a high concentration of nitrogen in the form of Ti-N species (i.e., those prepared with a N₂ percentage of 95% or above) present a loss in transmission that has been associated with the formation of oxygen vacancies (associated with Tiⁿ⁺ species, $n < 4$, detected by XPS) that would be responsible for a wide absorption extending over a large zone of the visible spectrum.^{21,61} The decrease in the resistivity of these films (cf. Supporting Information S7) confirms that these films are oxygen defective, again suggesting that incorporation of Ti-N species becomes favored by the presence of oxygen vacancies.^{25,34,54}

4.2. DOS and Electronic Structure in N-TiO₂. The DOS calculations reported in section 3.4 account for the different phenomenological behaviors found for N-TiO₂ thin films depending on the type and concentration of the nitrogen species incorporated into the lattice. We have shown that the N_i and N_{si} defects, associated with the Ti-NO and Ti-ON species detected by XPS, give rise to localized electronic states in the gap above the valence band edge of the oxide. In previous works, Di Valentin et al.^{11,13,15} reached a similar conclusion by simulating the electronic structure of isolated N_i defect states. We have investigated the influence of interdefect distances on the electronic properties, in larger supercells. For a two-defect model simulating the incorporation of a high concentration of N_i species within the lattice (cf. Figures 9 and 10), we have also proved that the gap states do not become extensively mixed with the valence band levels of the oxide and keep a localized

character. This theoretical result supports the experimental findings by ellipsometry and UV-vis spectroscopy for the 85% N₂ sample (cf. Figure 7), where the presence of a localized harmonic oscillator at around 375 nm is required for a good fitting of the experimental curves. Unfortunately, our experimental protocol does not enable the incorporation of a high concentration of Ti-NO species without Ti-N species being also formed. This limitation might be explained by the calculated energies of formation of the different defect states (section 3.4). Even though, the good agreement between experimental and theoretical results supports the development of isolated states in the gap rather than a band gap narrowing in the samples prepared with 85% or a lower concentration of N₂ in the plasma gas.

A direct comparison between our experimental and theoretical results is possible when dealing with the N_s defect states (i.e., Ti-N species according to the notation used by the XPS analysis) where, particularly for the structures simulating a high concentration of this species, a substantial mixing between the valence band states and those pertaining to the nitrogen can be deduced from the calculated partial DOS curves (c.f. Figure 10). As an overall effect, it can be interpreted that this mixing produces a shift toward the visible of the valence band edge, in agreement with our experimental observations for the samples prepared with nitrogen-rich plasmas. As discussed in section 4.1, the different interpretation regarding the modifications of the gap that was outlined in previous theoretical^{11–15} and experimental⁵⁴ works might be connected with the fact that they simulate or interpret experiments with more separated Ti-N species. In this way, our description of the optical and electronic properties of N-TiO₂ systems with a high concentration of Ti-N species would be in a better agreement with the original suggestions of Asahi et al.¹ of a band gap narrowing than with those of these more recent works.

4.3. Wetting Photoactivity of N-Doped TiO₂. Visible photoactivity of N-doped TiO₂ thin films is a very elusive effect with somehow contradictory results in the literature, where the red-shift of the valence band edge has been taken sometimes as a sufficient evidence warranting reactivity under visible illumination.¹⁶ In recent works, it has been pointed out that although visible absorption is a required condition, it is not sufficient to ensure visible photoactivity of N-TiO₂. Moreover, different conditions seem to be required for photocatalysis and for light-induced wetting angle changes over flat surfaces of this material.⁶⁴ The former is a much more demanding process that, besides the presence of nitrogen species, requires that the nitrogen-modified titania is crystalline and complies with some additional structural conditions, such as the simultaneous presence of both anatase and rutile polymorphs in the photoactive material.²² Since most N-TiO₂ thin films prepared in the present work were amorphous, we have investigated the effectiveness of either Ti-N or Ti-NO species in inducing some kind of visible photoactivity by following the changes in wetting angle upon illumination with visible light. The experiments carried out with the N-TiO₂ thin films have shown that samples with a high concentration of Ti-N species do not show visible photoactivity and keep their original wetting angle even after a prolonged illumination with visible photons (cf. Figure 11). By contrast, films containing Ti-NO species do present some visible photoactivity, which was evidenced by a partial and progressive decrease in the water contact angle of ca. 50° from an original wetting angle of 98° to a wetting angle of 52° after 60 min illumination. This behavior, even if occurring with a slow rate, indicates that in the presence of this species visible

light is capable of photoactivating the surface of these titanium oxide samples. A thorough discussion of this kind of partial hydrophilic transformation of N-TiO₂ surfaces upon visible light irradiation can be found in ref 24.

Our theoretical and experimental results have shown that a small concentration of Ti-NO species in the films do not significantly modify the band gap of the oxide but induces some localized electronic states close to the band edge. Visible light excitation up to the conduction band of the electrons associated with these electronic states in the gap should render a conduction band electron and a localized hole in the gap state. We believe that the precise localized character of this photohole is the factor precluding a continuous operation of these films as a photocatalyst, as the mobility of these photoholes induced with visible light is rather limited.¹⁵ Indeed, for a continuous photocatalytic process to take place, the migration of both electrons and holes toward the surface is required, as it usually happens in undoped TiO₂ illuminated with UV light. In N-TiO₂ systems, migration toward the surface of the photoholes generated in the illuminated layer (i.e., on the order of a micrometer) can only take place if a continuous band-like state forms in the gap. This is not certainly the case in our samples with a low concentration of incorporated Ti-NO species. However, as previously discussed by us,²⁴ visible-light partial conversion of the surface hydrophilicity occurs by just activating the utmost atomic layers whereby only surface electron-hole pairs are involved in the transformation. Therefore, the point to be stressed here is that while Ti-NO species are able to induce this visible-light transformation, Ti-N species are not. This finding contrasts with the original proposal of Asahi et al.¹ and thereafter of other authors^{5,16} attributing the visible photoactivity of N-TiO₂ materials to the Ti-N species. However, it complies with more recent results stressing that for visible photoactivity to occur, Ti-NO-like species must be present.^{26,56}

5. Conclusions

The previous results have shown that by using the PECVD technique it is possible to obtain a large set of N-TiO₂ thin films where the amount and type of nitrogen can be tuned by controlling the working parameters during the deposition of the films. Thus, Ti-NO species are the only type of incorporated nitrogen species when the films were prepared with a relatively low concentration of nitrogen in the plasma gas. On the other hand, a high concentration of Ti-N species becomes incorporated into the films for nitrogen-rich plasmas.

DOS calculations of differently doped anatase model systems have provided a detailed description of the influence of the N states, Ti-N and Ti-NO (and the related one Ti-ON), on the electronic structure of N-TiO₂. It is found that in anatase with a relatively high concentration of Ti-N species the valence band edge shifts upward because of the mixing of the N atomic levels with the levels of the lattice atoms. Consequently, the absorption edge of the UV-vis absorption spectra is red-shifted as found experimentally. On the contrary, for the Ti-NO species the electronic levels of the interstitial nitrogen species remain localized, and no band gap narrowing occurs. Experimentally, this situation yields spectra whose absorption edges are not shifted but present a separated absorption oscillator close to it.

Films containing Ti-N species are not photoactive with visible light, even if they present a red-shifted absorption edge. Visible light wetting photoactivity is only observed in N-TiO₂ films with Ti-NO defect states. This observation has been related to the surface excitation of the electronic states associated with these species, which appear in the gap close to a virtually unmodified valence band edge.

Acknowledgment. We thank the Ministry of Science and Education of Spain (Projects MAT 2007-65764, MAT 2010-18447, MAT 2010-21228, and the CONSOLIDER INGENIO 2010-CSD2008-00023) and the Junta de Andalucía (Projects TEP2275/P09-TEP-5283/CTS-5189) for financial support. This work has been carried out within the EU project NATAMA (Contract No. 032583).

Supporting Information Available: Additional information referred to in the text as S1–S8. This material is available free of charge via the Internet at <http://pubs.acs.org>.

References and Notes

- (1) Asahi, R.; Morikawa, T.; Ohwaki, T.; Aoki, K.; Taga, Y. *Science* **2001**, *293*, 269.
- (2) Diwald, O.; Thompson, T. L.; Zubkov, T.; Goralski, E. G.; Walck, S. D.; Yates, J. T. *J. Phys. Chem. B* **2004**, *108*, 6004.
- (3) Nakano, Y.; Morikawa, T.; Ohwaki, T.; Taga, Y. *Appl. Phys. Lett.* **2005**, *86*, 132104.
- (4) Diwald, O.; Thompson, T. L.; Goralski, E. G.; Walck, S. D.; Yates, J. T. *J. Phys. Chem. B* **2004**, *108*, 52.
- (5) Yates, H. M.; Nolan, M. G.; Sheel, D. W.; Pemble, M. E. *J. Photochem. Photobiol. A: Chem.* **2006**, *179*, 223.
- (6) Thompson, T. L.; Yates, J. T. *Chem. Rev.* **2006**, *106*, 4428.
- (7) Emeline, A. V.; Kuznetsov, V. N.; Rybchuk, V. K.; Serpone, N. *Int. J. Photoenergy* **2008**, *2008*, article ID 258394.
- (8) Mitoraj, D.; Kisch, H. *Angew. Chem., Int. Ed.* **2008**, *47*, 9975.
- (9) Trenczek-Zajac, A.; Kowalski, K.; Zakrzewska, K.; Radecka, M. *Mater. Res. Bull.* **2009**, *44*, 1547.
- (10) Oropeza, F. E.; Harmer, J.; Egdel, R. G.; Palgrave, R. G. *Phys. Chem. Phys.* **2010**, *12*, 960.
- (11) Di Valentin, C.; Pacchioni, G.; Selloni, A.; Livraghi, S.; Giamello, E. *J. Phys. Chem. B* **2005**, *109*, 11414.
- (12) Livraghi, S.; Paganini, M. C.; Giamello, E.; Selloni, A.; Di Valentin, C.; Pacchioni, G. *J. Am. Chem. Soc.* **2006**, *128*, 15666.
- (13) Di Valentin, C.; Finazzi, E.; Pacchioni, G.; Selloni, A.; Livraghi, S.; Paganini, M. C.; Giamello, E. *Chem. Phys.* **2007**, *339*, 44.
- (14) Napoli, F.; Chiesa, M.; Livraghi, S.; Giamello, E.; Agnoli, S.; Granozzi, G.; Pacchioni, G.; Di Valentin, C. *Chem. Phys. Lett.* **2009**, *477*, 135.
- (15) Di Valentin, C.; Pacchioni, G.; Selloni, A. *Phys. Rev. B* **2004**, *70*, 085116.
- (16) Chen, X.; Burda, C. *J. Phys. Chem. B* **2004**, *108*, 15446.
- (17) Vyacheslav, N.; Kuznetsov, N.; Serpone, N. *J. Phys. Chem. B* **2006**, *110*, 25203.
- (18) Lei, Z.; Ma, G.; Liu, M.; You, W.; Yan, H.; Wu, G.; Takata, T.; Hara, M.; Domen, K.; Li, C. *J. Catal.* **2006**, *237*, 322.
- (19) Umebayashi, T.; Yamaki, T.; Itoh, H.; Asai, K. *Appl. Phys. Lett.* **2002**, *81*, 554.
- (20) Liu, B.; Wen, L.; Zhao, X. *Sol. Energy Mater. Sol. Cells* **2008**, *92*, 1.
- (21) Lin, Z.; Orlov, A.; Lambert, R. M.; Payne, M. C. *J. Phys. Chem. B* **2005**, *109*, 20948.
- (22) Romero-Gómez, P.; Rico, V.; Borrás, A.; Barranco, A.; Espinós, J. P.; Cotrino, J.; González-Elipe, A. R. *J. Phys. Chem. C* **2009**, *113*, 13341.
- (23) Nakamura, R.; Tanaka, T.; Nakato, Y. *J. Phys. Chem. B* **2004**, *108*, 10617.
- (24) Borrás, A.; López, C.; Rico, V.; Gracia, F.; González-Elipe, A. R.; Richter, E.; Battiston, G.; Gerbasí, R.; McSporran, N.; Sauthier, G.; Gyorgy, E.; Figueras, A. *J. Phys. Chem. C* **2007**, *111*, 1801.
- (25) Graciani, J.; Alvarez, L. J.; Rodríguez, J. A.; Fernández-Sanz, J. *J. Phys. Chem. C* **2008**, *112*, 2624.
- (26) Chen, C.; Bai, H.; Chang, Ch. *J. Phys. Chem. C* **2007**, *111*, 15228.
- (27) Borrás, A.; Cotrino, J.; González-Elipe, A. R. *J. Electrochem. Soc.* **2007**, *154*, 152.
- (28) Gracia, F.; Holgado, J. P.; González-Elipe, A. R. *Langmuir* **2004**, *20*, 1688.
- (29) Ahn, K.-H.; Park, Y.-B.; Park, D.-W. *Surf. Coat. Technol.* **2003**, *171*, 198.
- (30) Nakamura, M.; Kato, S.; Aoki, T.; Sirghi, L.; Hatanaka, Y. *Thin Sol. Films* **2001**, *401*, 138.
- (31) Song, X. M.; Gopireddy, G.; Takoudis, C. G. *Thin Solid Films* **2008**, *516*, 6330.
- (32) Song, X. M.; Takoudis, C. G. *J. Vac. Sci. Technol. A* **2007**, *25*, 360.
- (33) Xie, Q.; Yiang, Y. L.; Detavernier, C.; Deduysche, D.; Van Meirhaeghe, R. L.; Ru, G. P.; Li, B. Z.; Qu, X. P. *J. Appl. Phys.* **2007**, *102*, article no. 083521.
- (34) Graciani, J.; Nambu, A.; Evans, J.; Rodriguez, J. A.; Fernández-Sanz, J. *J. Am. Chem. Soc.* **2008**, *130*, 12056.
- (35) Barranco, A.; Cotrino, J.; Yubero, F.; Espinós, J. P.; Clerc, C.; Gonzalez-Elipe, A. R. *Thin Solid Films* **2001**, *401*, 150.
- (36) Kresse, G.; Hafner, J. *Phys. Rev. B* **1993**, *47*, 558–561.
- (37) Kresse, G.; Furthmüller, J. *Phys. Rev. B* **1996**, *54*, 11169–11186.
- (38) Kresse, G.; Furthmüller, J. *Comput. Mater. Sci.* **1996**, *6*, 15–50.
- (39) Wang, Y.; Perdew, J. P. *Phys. Rev. B* **1991**, *44*, 298.
- (40) Perdew, J. P.; Chevary, J. A.; Vosko, S. H.; Jackson, K. A.; Pederson, M. R.; Singh, D. J.; Fiolhais, C. *Phys. Rev. B* **1992**, *46*, 6671.
- (41) Kresse, G.; Joubert, J. *Phys. Rev. B* **1999**, *59*, 1758.
- (42) Monkhorst, H. J.; Pack, J. D. *Phys. Rev. B* **1976**, *13*, 5188–5192.
- (43) Solov'ev, I. V.; Anisimov, V. I.; Dederichs, P. H. *Phys. Rev. B* **1994**, *50*, 16861–16871.
- (44) Anisimov, V. I.; Aryasetiawan, F.; Lichtenstein, A. I. *J. Phys.: Condens. Matter* **1997**, *9*, 767.
- (45) Dudarev, S. L.; Botton, G. A.; Savrasov, S. Y.; Humphreys, C. J.; Sutton, A. P. *Phys. Rev. B* **1998**, *57*, 1505.
- (46) Calzado, C. J.; Hernández, N. C.; Fernández-Sanz, J. *Phys. Rev. B* **2008**, *77*, 045118.
- (47) Pearse, R. W. B.; Gaydon, A. G. *The Identification of Molecular Spectra*; Chapman & Hall, Ltd.: London, 1950.
- (48) Suraj, K. S.; Bharathi, P.; Prahlad, V.; Mukherjee, S. *Surf. Coat. Technol.* **2007**, *202*, 301.
- (49) Romero-Gómez, P.; Barranco, A.; Cotrino, J.; Espinós, J. P.; Yubero, F.; González-Elipe, A. R. Plasma Deposition of N-TiO₂ thin Films. In *Industrial Plasma Technology: Applications from Environmental to Energy Technologies*; Kawai, Y., Ikegami, H., Sato, N., Matsuda, A., Uchino, K., Kuzuya, M., Mizuno, A., Eds.; Wiley: Weinheim, Germany, 2010; p 349.
- (50) Lassaletta, G.; Fernández, A.; Espinós, J. P.; González-Elipe, A. R. *J. Phys. Chem.* **1995**, *99*, 1484.
- (51) Cong, Y.; Zhang, J.; Anpo, M. *J. Phys. Chem. C* **2007**, *111*, 6979.
- (52) López-Luke, T.; Wolcott, A.; Xu, L.-P.; Chen, Sh.; Wen, Z.; Li, J.; de la Rosa, E.; Zhang, J. Z. *J. Phys. Chem. C* **2008**, *112*, 1282.
- (53) Asahi, R.; Morikawa, T.; Hazama, H.; Matsubara, M. *J. Phys.: Condens. Matter* **2008**, *20*, 064227.
- (54) Batzill, M.; Morales, E. H.; Diebold, U. *Phys. Rev. Lett.* **2006**, *96*, 026103.
- (55) Chen, H.; Nambu, A.; Wen, W.; Graciani, J.; Zhong, Z.; Hanson, J. C.; Fujita, E.; Rodriguez, J. A. *J. Phys. Chem. C* **2007**, *111*, 366.
- (56) Dunnill, C. W. H.; Aiken, Z. A.; Pratten, J.; Wilson, M.; Morgan, D. J.; Parkin, I. P. *J. Photochem. Photobiol. A: Chem.* **2009**, *207*, 244.
- (57) Saha, N. C.; Tompkins, H. G. *J. Appl. Phys.* **1992**, *72*, 3072.
- (58) Swanepoel, R. *J. Phys. E* **1983**, *16*, 1213.
- (59) Irie, H.; Washizuka, S.; Watanabe, Y.; Kako, T.; Hashimoto, K. *J. Electrochem. Soc.* **2005**, *152*, E351.
- (60) Serpone, N.; Lawless, D.; Khairutdinov, R. *J. Phys. Chem.* **1995**, *99*, 16646.
- (61) Martin, N.; Besnard, A.; Sthal, F.; Vaz, F.; Nouveau, C. *Appl. Phys. Lett.* **2008**, *93*, 064102.
- (62) Zhu, J.; Ren, J.; Huo, Y.; Bian, Z. *J. Phys. Chem. C* **2007**, *111*, 18965.
- (63) Finazzi, E.; di Valentin, C.; Pacchioni, G.; Selloni, A. *J. Chem. Phys.* **2008**, *129*, 154113.
- (64) Rico, V.; Romero-Gomez, P.; Hueso, J. L.; Espinós, J. P.; González-Elipe, A. R. *Catal. Today* **2009**, *143*, 347.